ELSEVIER

Tectonophysics 274 (1997) 97–115

TECTONOPHYSICS

Polyphase history and kinematics of a complex major fault zone in the northern Taiwan mountain belt: the Lishan Fault

Jian-Cheng Lee [a,*], Jacques Angelier [b], Hao-Tsu Chu [c]

[a] *Institute of Earth Sciences, Academia Sinica, P.O. Box 1-55, Nankang, Taipei, Taiwan, ROC*
[b] *Géotectonique (URA 1759), Université P. & M. Curie, 4 place Jussieu, T26-25-E1, 75252 Paris, France*
[c] *Central Geological Survey, P.O. Box 968, Taipei, Taiwan, ROC*

Received 20 February 1996; accepted 2 September 1996

Abstract

The Lishan Fault is a major fault zone in the Taiwan collision belt. It separates two major units, the Hsüehshan Range and the Backbone Range, which differ in lithology, ages of sediments, metamorphic grades and deformation styles. Despite the importance of the Lishan Fault, its evolution and tectonic behaviour remained poorly known and controversial. We therefore carried out a tectonic study which includes both the identification of structures in and along the fault zone and the palaeostress analysis aiming at reconstructing the succession of fault mechanisms. The Lishan Fault zone underwent polyphase evolution with reactivations under different tectonic regimes, consistent with the Cenozoic history of Taiwan.

(1) On the Hsüehshan Range, the earliest events reflect the Palaeogene–Miocene extension of the Chinese continental margin.

(2) Serial cross-sections and observation of ductile–brittle structures show east-vergent folding, indicating that for the most recent compressional evolution related to late Cenozoic Taiwan collision the Lishan Fault was a steeply dipping east-vergent back-thrust. The compression occurred along NW–SE trends, inducing thrusting, but also along N–S ones, inducing transpression with reverse sinistral slip. The Lishan Fault thus underwent contraction as well as strike slip during the mountain building of the Taiwan orogeny. Reverse and strike-slip fault systems alternated because of permutations σ_2/σ_3 under the same compressional stress regime of NW–SE σ_1. Minor compressional events also occurred.

(3) A late extension, accommodated by normal faulting, reveals the influence of both the N–S extension in the Okinawa Trough northeast off Taiwan.

Keywords: fault; deformation; polyphase; Taiwan; paleostress

1. Introduction

The Lishan Fault zone trends parallel to the major NNE-trending grain of the Taiwan mountain belt (Fig. 1). It corresponds to two major valleys, the Lanyangchi valley to the north and the Tachiachi valley to the south, the water divide being 20 km north of Lishan. The Lishan Fault zone separates two major geological provinces: the Hsüehshan Range to the west and the Backbone Range to the east (Fig. 1).

Major differences between the Hsüehshan Range and the Backbone Range are highlighted by the contrasts in lithologies, ages of rock formations, grades of metamorphism and styles of deformation. The Hsüehshan Range is composed of Palaeogene continental margin sediments, mostly Eocene and Oligocene in age (Table 1). The Backbone Range consists of Palaeogene to Neogene pelitic sediments,

* Corresponding author. E-mail: jclee@earth.sinica.edu.tw

0040-1951/97/$17.00 © 1997 Elsevier Science B.V. All rights reserved.
PII S0040-1951(96)00300-9

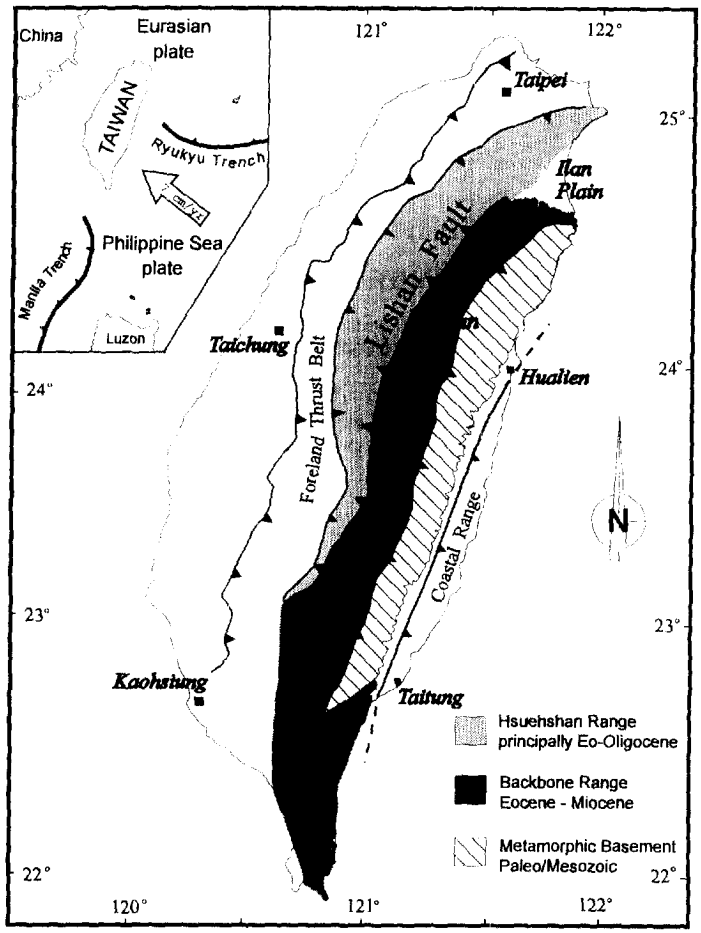

Fig. 1. Tectonic setting of Taiwan and general geological provinces in the Lishan Fault area (after Ho, 1988).

Eocene to Miocene in age (with a hiatus of the Oligocene formations in northern Taiwan; see Teng et al., 1991). Along the Lishan Fault zone, the Oligocene massive sandstone and slate formations of the Hsüehshan Range are in contact with the Miocene slate formation of the Backbone Range.

In general, the metamorphic grade in the Taiwan mountain belt increases from west (the foreland) to east. The prehnite–pumpellyite facies is present in the western Hsüehshan Range whereas the upper greenschist facies is represented in the eastern Hsüehshan Range (Liou, 1981; Chen et al., 1983b). However, east of the contact between the Hsüehshan Range and the Backbone Range, lower metamorphic grade facies (prehnite–pumpellyite facies) are found in the western Backbone Range (Chen et al., 1983b; Chen, 1984; Liu, 1988; Hsieh, 1990). A major discontinuity thus occurs in the distribution of metamorphism between the Hsüehshan Range and the Backbone Range, corresponding to the location of the present Lishan Fault zone.

Concerning the style of the late Cenozoic deformation, the pop-up structure (Clark et al., 1993; Chu et al., 1996), symmetric folds and coaxial strain deformation (Tillman and Byrne, 1995) prevailing in the Hsüehshan Range was not observed in the Backbone Range, which by contrast is generally characterized by asymmetric folds with west-vergent shear structures and noncoaxial strain deformation.

Outcrops along the Lishan Fault are discontinuous and often difficult to access; in addition, similar slate formations are present on both sides of the southern

Table 1
Stratigraphic units and their lithology, Lishan Fault area, northern Taiwan

Stratigraphic unit	Age	Lithology
Hsüehshan Range, Meichi Sandstone	Late Oligocene	Medium- to fine-grained sandstone or quartzite, with intercalated shale or argillite
Hsüehshan Range, Szeleng Sandstone	Oligocene	Coarse-grained massive sandstone or quartzite, with intercalated thin layers of shale or argillite
Hsüehshan Range, Chiayang Formation	Oligocene	Slate, sometimes with thin layers of psammite
Hsüehshan Range, Tachien Sandstone	Eocene	Coarse-grained massive sandstone or quartzite
Backbone Range, Lushan Formation	Late Oligocene to Miocene	Slate, sometimes with sandstone layers

segment of the Lishan Fault zone, which makes geological mapping difficult. Field observations across the Lishan Fault zone were carried out based on mapping and geothermal investigation (Tseng, 1978), as well as study of metamorphism (Chen, 1979; Chen et al., 1983b). All these studies, however, did not aim at elucidating the tectonic behaviour of the Lishan Fault zone. Studies of the seismicity distribution and analyses of earthquake focal mechanisms (Tsai, 1975; Wu, 1978; Yeh et al., 1991) revealed that the Lishan Fault is seismically active, with an extensional tectonic regime prevailing at the northern tip, near the Ilan Plain (Fig. 2).

Although the Lishan Fault is one of the largest features of the Taiwan mountain belt (Biq, 1971; Ho, 1986a,b, 1988), its significance remains unclear. The linear trace, juxtaposition of contrasting rock units (at least in the northern and central part), contrast in metamorphic grades and presence of fractured cataclastic rocks leave little doubt that the Lishan Fault represents a major shear zone. However, the absence of reliable markers of displacement across the shear zone made the determination of the sense and amount of displacement difficult. As a consequence, the structural interpretation is controversial. The Lishan Fault has previously been interpreted as an oblique left-lateral shear zone with a west-verging reverse component of motion (Biq, 1971; Wu, 1978). Stratigraphic studies revealed a significant contrast between the formations on the western (Hsüehshan Range) and eastern (Backbone Range) sides of the fault; this contrast was attributed to the presence of a major normal fault during the Oligocene (Teng et al., 1991).

Recently, strain analysis in the Hsüehshan Range of central Taiwan (Clark et al., 1993; Tillman and Byrne, 1995) suggested the presence of an east-vergent back-thrust structure in the Lishan Fault zone, forming the eastern boundary of the Hsüehshan Range which exhibits a pop-up structure. However, Crespi et al. (1996) suggested that the Lushan Formation of the Backbone Range (east of the Lishan Fault) is affected by N–S-trending normal faulting, based on field observation.

In summary, the Cenozoic structure of the Lishan Fault reveals contradictory aspects in that it shows contrasting evidences of being a major normal fault, a major reverse fault, and also a sinistral strike-slip fault. Furthermore, although the Lishan Fault was classically interpreted as an old fault bounding an extensional basin of the Chinese continental margin (Teng et al., 1991), a new interpretation of the whole Central Range of Taiwan suggested that the Lishan Fault zone was a major suture zone during the Late Miocene, between the Chinese continental margin and an accretionary prism corresponding to the present Backbone Range (Lu and Hsü, 1992).

Because of its major role in the mountain building of Taiwan, the structural evolution of the Lishan Fault deserves particular consideration. In this paper, we combine field observation of geological structure and regional palaeostress analyses, in order to better describe the Lishan Fault zone and to understand its tectonic behaviour. Our study concentrates on the northern and the central part of the Lishan Fault (Fig. 2a), where massive sandstones provide good stratigraphic markers within the Hsüehshan Range, in contrast with the slates of the Backbone Range.

2. The Lishan Fault zone: stratigraphy and structure

The geological structures in the Lishan Fault area are principally characterized by folds and faults on

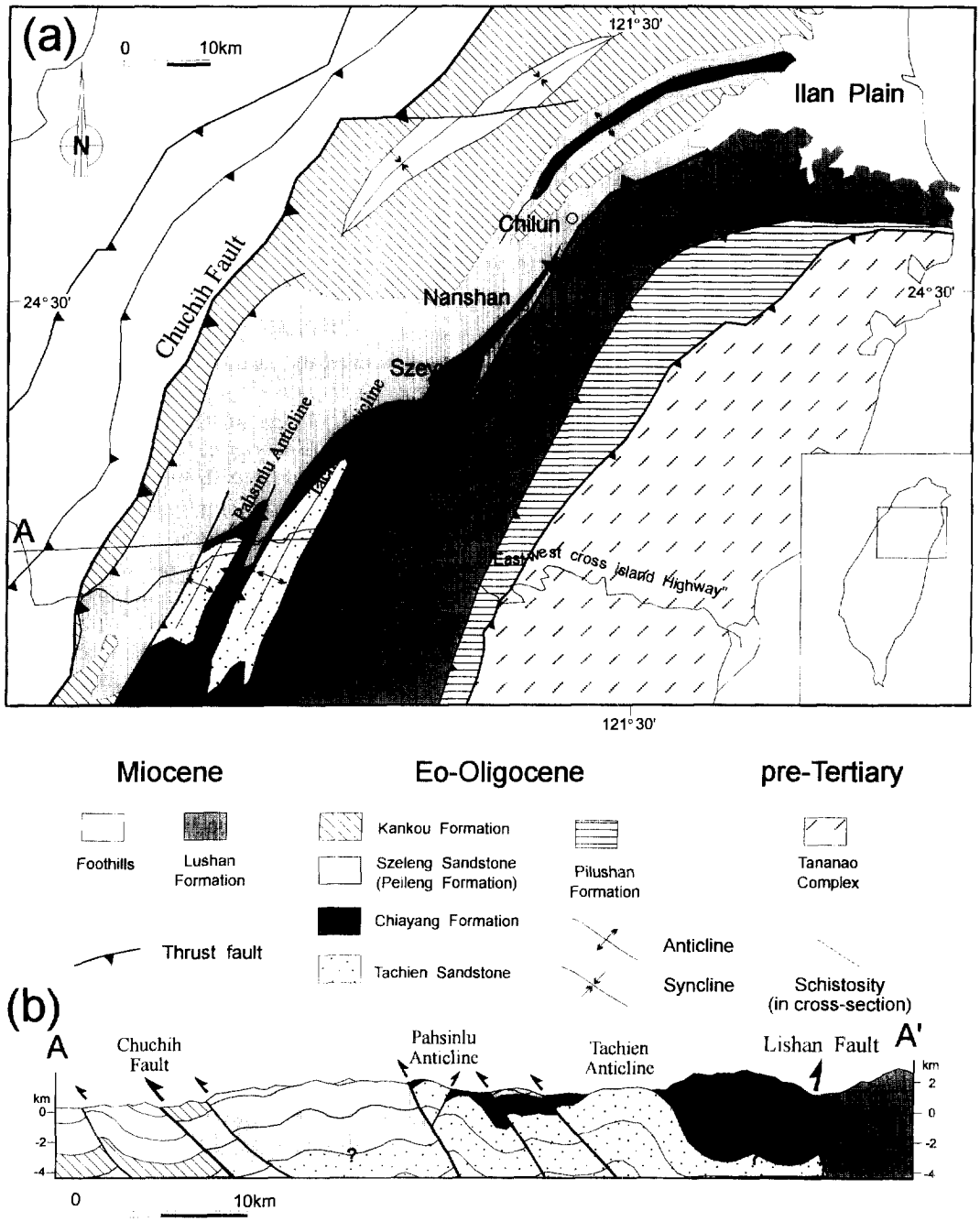

Fig. 2. (a) Geological map of the Lishan Fault region (after Ho, 1986b). (b) Cross-section (*A*–*A'*, see location in a).

both sides (Hsüehshan Range and Backbone Range). The geological cross-section of Fig. 2b illustrates the general structure across the Lishan Fault zone. The names of formations, which are not discussed in the text, are described in Fig. 2 and Table 1.

2.1. The Hsüehshan Range

On the western side of the Lishan Fault, Palaeogene formations of massive sandstone are about 950 m thick to the north (the Szeleng Sandstone; Huang and Lee, 1992) and 2000 m thick to the south (the Tachien Sandstone; Chen, 1979; Lee, 1987). Their presence makes structural analysis easier in the Hsüehshan Range, revealing a succession of folds truncated by faults (Fig. 2b). These sandstones, Eocene (Tachien) to Oligocene (Szeleng) in age, are the oldest rock formations in this area. According to Chen (1977, 1979, 1992), a significant change in facies occurs from north to south in the Hsüehshan Range, the sediment grain size being finer to the south. As a consequence, the rock formations which are in tectonic contact with the Backbone Range change from sandstone (in the northern part of the study area) to slate (in the southern part).

Above these sandstone formations, there is a sequence of slates and interbedded slates and psammites, with a change in facies (the sediments being generally finer to the southeast). These slate formations are affected by narrowly spaced folds and faults. Near the base, however, the structures resemble those of the underlying sandstone formation; the wavelength of the fold decreases generally upward because of the change in lithology (Fig. 2b). In this slate formation, the cleavage is well developed and is often nearly vertical. A recent structural analysis of the Hsüehshan Range (Chu et al., 1996) indicated that the overall structure is characterized by repeated pop-up structures with folding and thrusting verging both to the east and to the west.

2.2. The Backbone Range

On the eastern side of the Lishan Fault in the study area (Fig. 2a), the Neogene slate formation is composed of black or grey slates with occasional intercalation of psammite layers. This Lushan Formation is characterized by a tight slaty cleavage dipping steeply to moderately to the southeast; shear zones contain numerous folded quartz and calcite veins. On a wider scale, the Lushan Formation reveals a regular west-vergent shear structure. The deformation pattern, however, differs from that of the adjacent Hsüehshan Range, with tighter folds and two main cleavages (instead of a single one in the Hsüehshan Range).

Because fossils are scarce, the age range of the Lushan Formation is still not accurately defined. A Miocene age (N6–N9 zones) was determined by fossils in the upper part near the contact with the Hsüehshan Range (Chang, 1971, 1974, 1976). As for the lower part, in the absence of stratigraphic data, a Late Oligocene age cannot be excluded (Chen, 1977, 1992).

2.3. Reconstruction of serial cross-sections

The geological sections of Fig. 3 describe the structure of the Lishan Fault zone, over a distance of about 60 km from Niuto to Lishan. They were built based on direct observation in outcrops, that is, with little extrapolation. They are presented below from north to south.

Near Niuto (profile *A–A′*, Fig. 3), the Palaeogene massive sandstone (Hsüehshan Range) forms a gentle anticline across the valley. East of this anticline, the Neogene slate formation (Backbone Range) crops out and dips steeply to the southeast. The contact between the two lithological units, which is difficult to observe because of vegetation, is probably a shear zone, as indicated by the presence of fractured blocks. Two kilometres farther south (profile *B–B′*, Fig. 3), the Palaeogene sandstone and the Neogene slate formation are separated by the valley alluvium (about 300 m wide). A shear zone was observed on the eastern border of the Palaeogene sandstone, containing broken rocks and many striated fault surfaces. It implies the existence of a strong deformation concentrating between these two units.

Near Chilun, two profiles (*C–C′* and *D–D′*, Fig. 3) show that the anticline of Palaeogene sandstone of the Hsüehshan Range constitutes an east-vergent fold. On the Backbone Range, the slate formation dips steeply to the southeast as before. Within the anticline of the Palaeogene sandstone, fault striations and quartz veins (sometimes arranged en échelon), indicate brittle deformation associated with folding in this shear zone. The various natures and orientations of brittle structures illustrate the complexity of the tectonic history of the Lishan Fault, requiring special analysis (discussed in the next section).

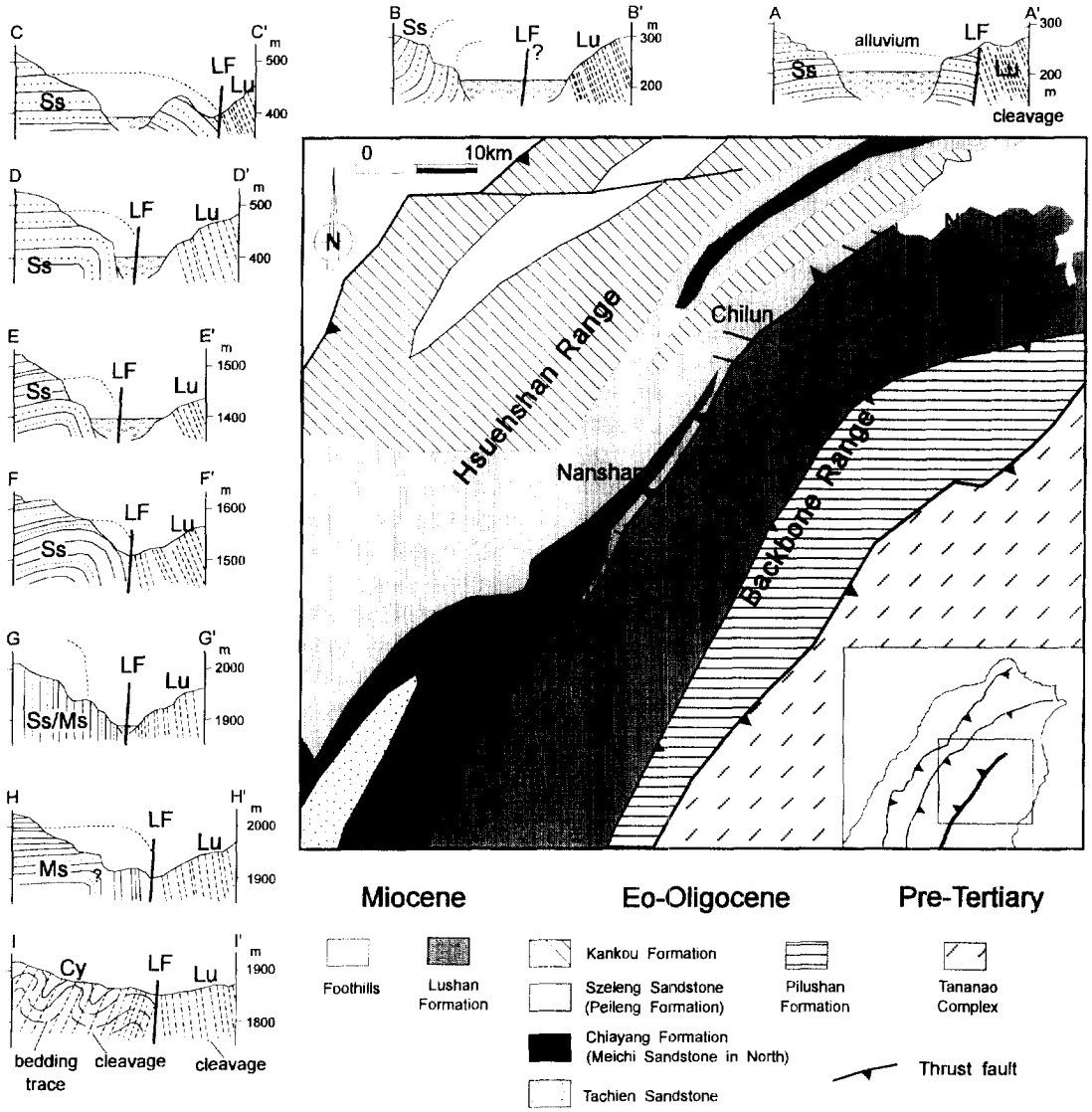

Fig. 3. Serial cross-sections across the Lishan Fault zone. Sections: *Ss* = Szeleng Sandstone; *Ms* = Meichi Sandstone; *Cy* = Chiayang Formation; *Lu* = Lushan Formation. For details see Table 1.

Near Nanshan (profiles *E–E′* and *F–F′*, Fig. 3), the structure remains similar to that of profiles *C–C′* and *D–D′*, the bedding planes near the contact between the massive sandstone and the slate formation being almost vertical. The contact itself is represented by a shear zone with numerous fractured blocks. This shear zone dips very steeply to the northwest (profile *F–F′*, Fig. 3). At a short distance to the south, near Szeyuan (profile *G–G′*, Fig. 3), the contact between the Hsüehshan Range and the Backbone Range shows nearly vertical bedding planes. All these sections show a large east-vergent flexure zone which becomes tighter to the south (Fig. 3).

Near Wuling, half-way between Nanshan and Lishan (profile *H–H′*, Fig. 3), a sandstone formation with interbedded slates replaces the massive sandstone, as a result of the change in facies along the Hsüehshan Range (Chen, 1979; Chen et al., 1983a).

This formation is folded as an east-vergent anticline, similar to that of profile *D–D'*. Outcrops are scarce along the contact; however, at a short distance to the east, the black slate of the Lushan Formation dips steeply to the southeast.

Finally, near Lishan (profile *I–I'*, Fig. 3), another facies of the Oligocene rock formation in the Hsüehshan Range (the Chiayang Formation, see Table 1), which consists of slates and interbedded psammites, is in contact with the Neogene slate formation of the Backbone Range. As a result, the contrast in lithology observed in the sections presented above is absent and the structural analysis is more difficult. However, we could identify east-vergent folding and shearing in the Chiayang Formation of the Hsüehshan Range, based on the relationship between bedding and slaty cleavage as well as on the presence of S/C fabrics. These aspects are illustrated in a local cross-section (Fig. 4).

2.4. Structure of the Lishan Fault

The reconstruction of these nine serial cross-sections across the Lishan Fault zone (Fig. 3), in addition to scattered observations, led us to the conclusions listed below:

(1) On the western side of the Lishan Fault (the Hsüehshan Range), a gradual facies change occurs within the Palaeogene sediments. From north to south, thick layers of massive sandstone (the Szeleng Sandstone) change progressively to series of interbedded sandstones and slates (the Meichi Sandstone) and possibly to slates (the Chiayang Formation) in the southern part of the studied area. On the eastern side of the Lishan Fault (the Backbone Range), the Miocene slate Lushan Formation crops out continuously. This contrast in lithology and age across the Lishan Fault zone suggests that during the Palaeogene and the Miocene the Lishan Fault already represented a major discontinuity between the present Hsüehshan and Backbone ranges. As far as its oldest history is concerned, it is of importance to keep in mind that this major discontinuity has been interpreted in two contrasting ways: a simple basin boundary within the Chinese continental margin (Teng et al., 1991), or a domain undergoing subduction at the front of an accretionary prism and finally becoming a suture zone during the Late

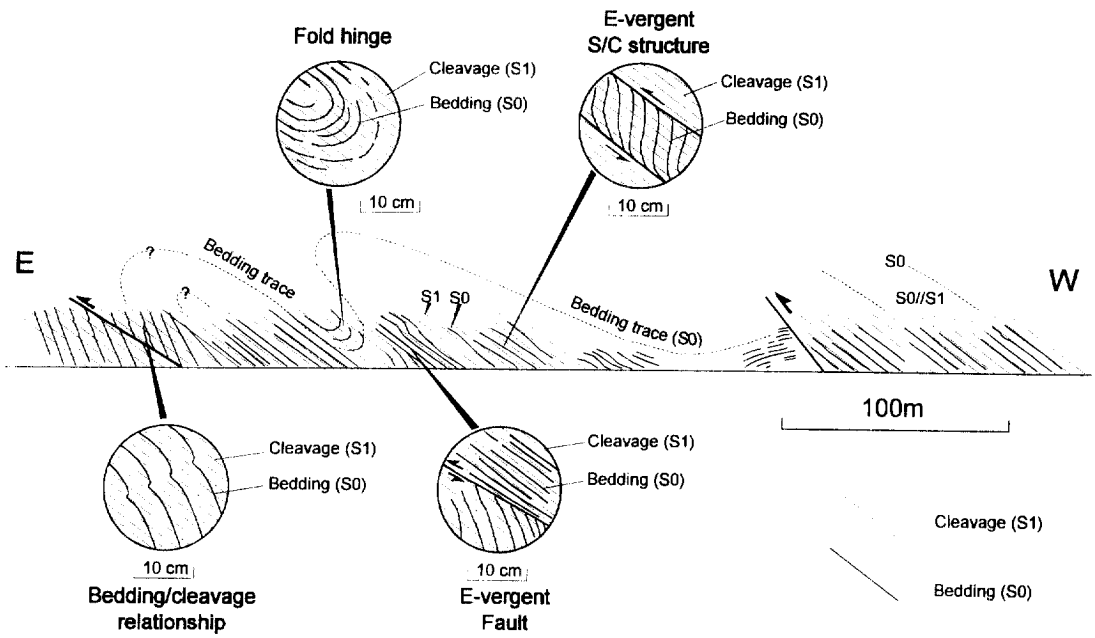

Fig. 4. Field section showing east-vergent folding and shearing structures along the East–West Cross-Island Highway, west of the Lishan Fault (location in Fig. 2) in the Chiayang Formation. Note the relationship between bedding, metamorphic cleavage, fold, reverse faulting and S/C shear fabrics.

Miocene (Lu and Hsü, 1992). Details will be discussed in a later section.

(2) An east-vergent shear zone of back-folding and back-thrusting follows the eastern border of the Hsüehshan Range. Such back-folding and back-thrusting is known elsewhere in the Taiwan mountain belt, especially in the Central Range including the Backbone Range and the Pre-Tertiary Basement (Fig. 1), although west-vergent structures consistent with generally westward transportation dominate (this is the case for most major thrust faults in the Taiwan belt). The western Hsüehshan Range is thrusted to the west, especially near the Chuchih Fault (Fig. 2). In contrast with this general attitude, we observed east-vergent folding and flexuring on the eastern side of the Hsüehshan Range, near the Lishan Fault zone (as most profiles of Fig. 3 show).

(3) The nearly vertical attitude of the bedding and the cleavage along the Lishan Fault zone (Fig. 3) indicates that the dip of the Lishan Fault is nearly vertical on the surface. The east-vergent shearing structures prevailing on the western side of the Lishan Fault infer that the fault is dipping steeply to the west. On the other hand, the cleavage which is vertically to steeply dipping to the east on the eastern side of the Lishan Fault (Fig. 3) shows that the fault had probably initiated as west-vergent with a dip to the east. Thus this structural geometry suggests that the contact of the Hsüehshan Range and the Backbone Range corresponds to a boundary which limited the east-vergent structures, and a zone of back-thrusting dipping steeply to the west near the surface and the dip of the fault plane may turn to the east in the deep down (Fig. 2b).

(4) The Lishan Fault has a complicated tectonic history, as revealed by the variety of brittle and ductile structures in nature and orientation. This late Cenozoic tectonic evolution included extensional regimes (the oldest ones may correspond to the evolution of the Chinese continental margin) as well as compressional regimes (the most recent ones being related to the Plio–Pleistocene collision). In order to decipher this structural complexity, the structural analysis presented above will not suffice. A specific tectonic analysis was consequently undertaken.

3. Tectonic analysis along the Lishan Fault

Numerous structures related to brittle deformation were observed along the Lishan Fault zone. Systematic orientation data were collected at sites where the bedrock crops out in the absence of landslides.

A 400 m long cross-section in the Chiayang slate Formation of the Hsüehshan Range near Lishan (Fig. 4) is first presented to illustrate the characteristics of ductile–brittle deformation. East-vergent shearing is characterized by bedding/cleavage relationships, S/C fabrics, and east-vergent folds and faults. These features are consistent not only with the larger structures (Fig. 3), but also with the pyrite pressure shadow shearing structures indicating east-vergent shear at the microscopic scale in this area (Clark et al., 1993).

Systematic analyses of brittle structures were carried out along the Lishan Fault, in order to identify the palaeostress states related to tectonic mechanisms within this fault zone. A brittle shear zone was observed at several places along the Lishan Fault valley, and numerous folds, faults and fractures were analysed within this shear zone. We describe below the characteristics of fractures, and we present the criteria used to establish the tectonic chronology, before discussing the results of the tectonic analysis.

Regarding the methods, we first adopted the usual tectonic interpretation in structural geology (e.g., Dunne and Hancock, 1994). Good examples of significant features along the Lishan Fault zone are the sets of large quartz veins indicating perpendicular tensile effective stress, or the en échelon pattern of smaller sigmoidal quartz veins indicating shear. However, specific methods were required to decipher the polyphase brittle evolution of the Lishan Fault zone.

3.1. Methods for palaeostress determinations

A more complete reconstruction of palaeostresses was obtained through inverse methods which allow reconstruction of palaeostress tensors using sets of fault-slip data. Such an analysis is based on the concepts of mechanical relationships between brittle features (especially striated faults) and palaeostress. During the last decades, this has proved to be successful for the identification and characterization of

tectonic events (Angelier, 1984, 1990), and was thus extensively used to interpret fault-slip patterns.

In summary, based on the stress–slip relationships in faulted media undergoing small brittle deformation, a reduced stress tensor is calculated for each tectonic regime provided that the size and variety of the fault-slip data set collected allows application of the least-square techniques. Four variables are thus determined, which describe the orientation of the three principal stress axes σ_1, σ_2, and σ_3 and the ratio between principal stress differences, $\Phi = (\sigma_2 - \sigma_3)/(\sigma_1 - \sigma_3)$. This ratio plays an important role in stress–shear relationships. Note that σ_1 is the maximum compressional stress while σ_3 is the minimum stress (compression being considered positive).

The assumption that for a given event and a given rock mass all faults moved independently but consistently under a single homogeneous stress regime expressed by a unique stress tensor is an approximation. Data collection involves errors, dispersion occurs in local stress patterns, the presence of weakness zones induces stress perturbation, and faults movements influence one another mechanically and geometrically. A theoretical evaluation of such effects was made based on distinct-element analysis by Dupin et al. (1993), showing that dispersion remains generally small provided that fault-slip data sets are large and include a variety of orientations. Similar conclusions had been obtained empirically, resulting from local and regional applications which revealed that the average misfit between observed fault slips and calculated shear vectors on fault planes remains generally small, within the range of measurement and observation uncertainties. Thus, for a given tectonic event, stress fields can be reliably reconstructed on the regional scale, based on the compilation of local determinations of stress tensors.

In practice, one searches for the best fit between all slip data collected in a rock mass which experienced faulting. Some examples of such determinations are shown in Figs. 5 and 6. Misfit estimators deserve special attention because they allow evaluation of the reliability of the results. The nature and significance of misfits are discussed extensively elsewhere (Angelier, 1990). In this paper, for convenience, the misfits for each tensor determination are summarized in Table 2 through a single-quality estimator, from A (excellent) to D (poor). Stress tensor determinations along the Lishan Fault were generally acceptable. The qualities range only from B to D, but consistency of the results at various sites induces confidence in the results. Consideration of tension data, such as for mineral veins, provided useful additional information.

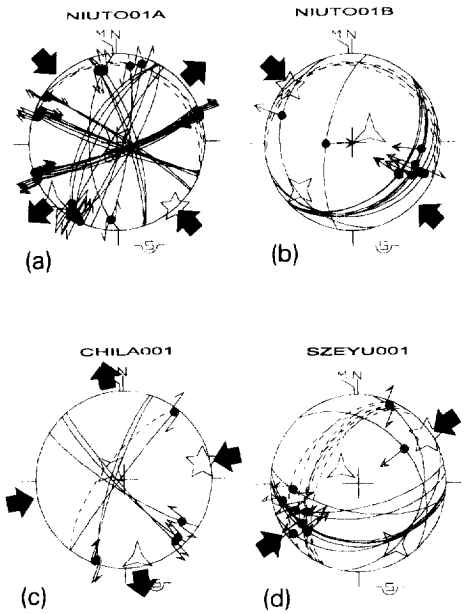

Fig. 5. Examples of stress tensor determination in the area of the Lishan Fault. Stereoplots: Schmidt's projection, lower hemisphere. Bedding planes shown as dashed-line great circles. Fault planes shown as thin-line great circles, with slickenside lineations as dots with arrows indicating the sense of motion (inward direction for reverse slip). Computed stress axes shown as 5-point stars (σ_1), 4-point stars (σ_2), and 3-point stars (σ_3). Method of calculation of stress tensor after Angelier (1984). (a) Major NW–SE compression, strike-slip faulting (Niuto, location in Fig. 7). (b) Major NW–SE compression, reverse faulting (same site). (c) Minor NE–SW compression, strike-slip faulting (Chilun, location in Fig. 7). (d) Minor NE–SW compression, oblique reverse faulting (Szeyuan, location in Fig. 7 and backtilting in Fig. 6c). Numerical results given in Table 2.

Dilatant veins and striated faults were observed. The horizontal surface of each studied site is less than 0.5 km^2. Faults and veins were easily identifiable due to the presence of slickenside lineations and mineral infills (in most cases quartz). Systematic collection of orientation data was carried out for bedding surfaces, faults and slip vectors indicated by striae and veins. A crucial aspect in the collection of data was the de-

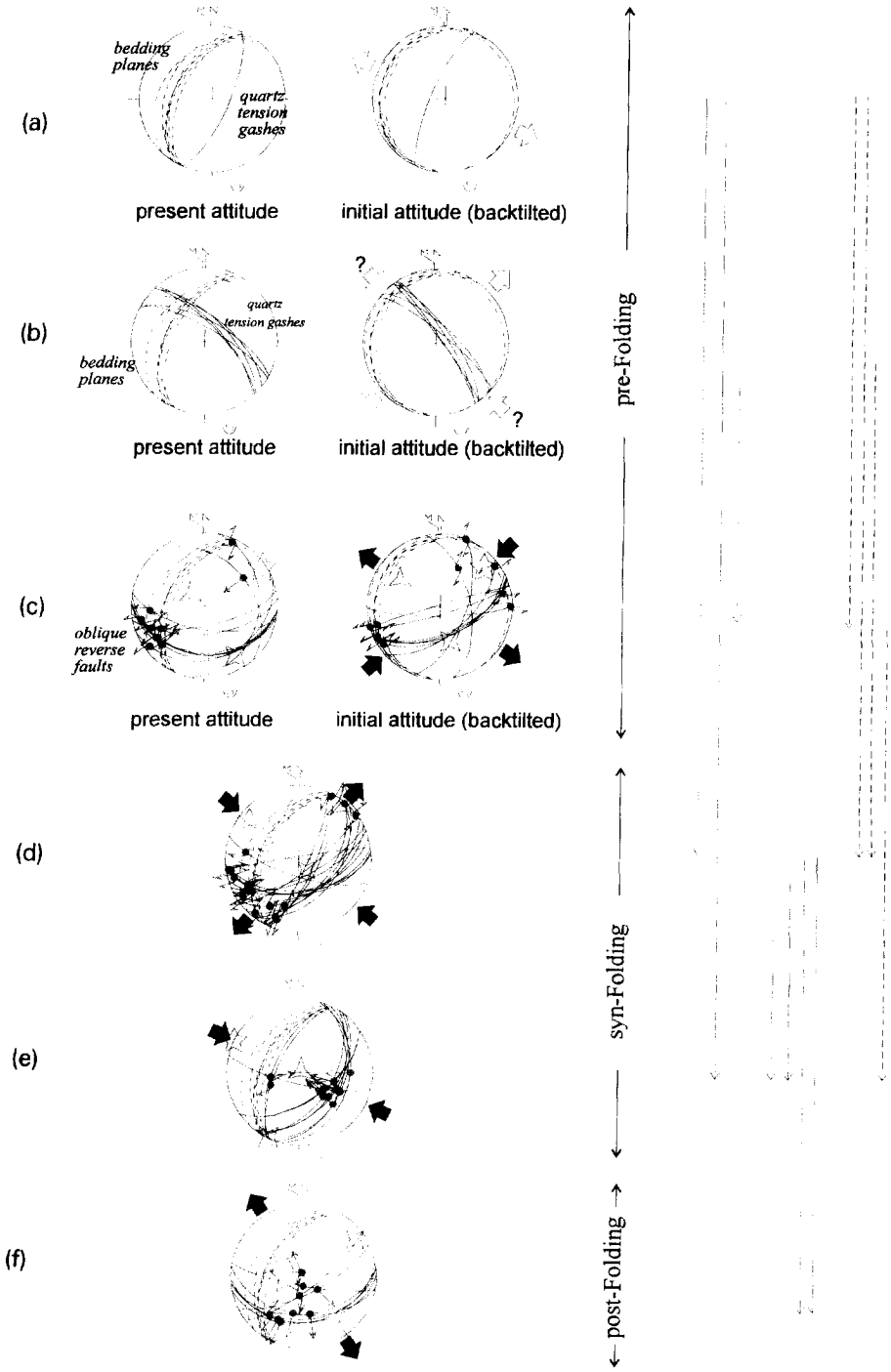

Fig. 6. Evolution of brittle tectonics and palaeostress reconstructions at Szeyuan. Location in Figs. 2 and 7. Stereoplots: Schmidt's projection, lower hemisphere (symbols as for Fig. 5). Back-tilting shown for pre-folding patterns. (a) Quartz veins, WNW–ESE extension. (b) Quartz veins, NE–SW extension or NW–SE compression. (c) Tilted strike-slip faults, minor NE–SW compression. (d) Strike-slip faults, main NW–SE compression. (e) Reverse faults, main NW–SE compression. (f) Normal faults, late NW–SE extension. On the right-hand side, thin solid-line arrows (sense from older to younger) indicate relative chronology at this site while thin dashed-line arrows summarize relative chronology at other sites.

Table 2
Results of palaeostress analysis along the Lishan Fault

Site ref.	Formation affected	Latitude (N)	Longitude (E)	Axis σ_1		Axis σ_2		Axis σ_3		Φ	N	Q
				tr	pl	tr	pl	tr	pl			
NIUTO01A	Szeleng	24°38′	121°33′	139	1	18	88	229	1	0.72	32	B
NIUTO01B	Szeleng	24°38′	121°33′	317	3	226	14	59	76	0.71	13	C
NIUTO01C	Szeleng	24°38′	121°33′	272	12	29	65	178	22	0.41	39	B
NIUTO002	Szeleng	24°37′30″	121°33′	344	7	74	3	186	82	0.47	4	D
NIUTO002	Szeleng	24°37′30″	121°33′	258	23	350	6	94	67	0.73	8	D
CHILA001	Szeleng	24°34′30″	121°27′42″	79	10	309	75	171	12	0.48	6	D
CHILA003	Szeleng	24°34′30″	121°27′42″	136	2	281	87	46	2	0.44	7	D
CHILA005	Szeleng	24°34′30″	121°27′42″	294	1	202	69	24	21	0.53	7	D
TULIN001	Lushan	24°25′	121°21′24″	101	12	335	70	194	15	0.51	16	C
TULIN02A	Szeleng	24°25′	121°21′24″	360	2	92	51	268	38	0.16	7	D
TULIN02A	Szeleng	24°25′	121°21′24″	277	13	185	10	59	74	0.51	13	D
TULIN02B	Szeleng	24°25′	121°21′24″	127	16	312	73	217	1	0.61	9	D
SZEYU001	Szeleng	24°23′	121°20′30″	56	6	149	20	309	69	0.41	10	D
SZEYU001	Szeleng	24°23′	121°20′30″	309	15	143	75	40	4	0.92	17	C
SZEYU001	Szeleng	24°23′	121°20′30″	295	1	205	2	46	88	0.59	11	D
SZEYU001	Szeleng	24°23′	121°20′30″	270	72	54	15	147	10	0.15	9	D
WULIN001	Meichi	24°21′	121°18′54″	107	9	275	81	17	2	0.42	16	C

Trends and plunges of the principal stress axes in degrees. N = number of measurements; Q = quality of the results of the calculated tensor (decreasing from A to D).

termination of slip senses, which was done based on offsets of layers as well as on several criteria reported in the literature (Petit, 1987; Angelier, 1994).

From the tectonic point of view, it is extremely important to distinguish brittle structures related to distinct tectonic regimes, and it is even more important to separate structures resulting from different tectonic events. A single tectonic event may correspond to two or more stress regimes, and the distribution of palaeostress trends for a given event may be affected by stress permutations (a phenomenon which occurred along the Lishan Fault zone, as discussed in a later subsection). Before discussing the chronological aspects of the tectonic history of the Lishan Fault zone as revealed by palaeostress analysis, it is worthwhile to present the main regimes that could be identified.

3.2. Main palaeostress regimes

The Lishan Fault zone is characterized by polyphase deformation. The most important deformation event observed in the field is represented by veins, folds, joints, and faults, all compatible with a maximum compressional stress (σ_1) trending NW–SE and nearly horizontal. Note that this orientation of compression is consistent with the overall mechanism of the Plio–Pleistocene collision of Taiwan.

The oldest fractures that we have found in this area are quartz veins. Some of these veins strike approximately NE–SW and reveal a NW–SE-trending minimum stress (σ_3). They are associated with some extensional shearing (few normal faults and en échelon veins). Most quartz veins, however, strike approximately NW–SE and indicate a NE–SW-trending minimum stress (σ_3), compatible with a widespread NW–SE compression.

Strike-slip faults are common. Two main regimes of strike-slip faulting were identified in the field. They are illustrated in the stereonets of Fig. 5. The main phase of strike-slip faulting corresponds to a σ_1 axis trending NW–SE (Fig. 5a). The associated structures are well distributed along the Lishan Fault valley. We have separated the faults into two groups: inherited and neoformed faults. The neoformed strike-slip faults (i.e., fault planes newly formed under this regime) are characterized by conjugate strike-slip patterns (with most dextral faults trending WNW–ESE and most sinistral ones trending N–S). Inherited strike-slip faults, corresponding

to reactivation of pre-existing weakness planes, are also present, revealing earlier tectonic episodes and resulting in a variety of orientations (Fig. 5a). Some other strike-slip fault systems (dextral along NE–SW trends and sinistral along NW–SE ones) are also present, corresponding to an episode with σ_1 trending E–W to ENE–WSW (Fig. 5c). They reveal a minor tectonic phase.

As for the reverse faults, two principal systems of reverse faults were also identified. A major compressional tectonic event is represented by conjugate reverse faults: the corresponding σ_1 axes trend N120°E to N140°E (Fig. 5b). This compressional tectonism is clearly coeval with the NW–SE compression revealed by strike-slip fault systems. Another compressional event, which is minor, is characterized by systems of conjugate reverse faults observed in a single site; it is consistent with a NE–SW-trending σ_1 axis (Fig. 5d). Although strike-slip and reverse fault systems were often found in separate sites, here the two main compressional trends are in fact found to be identical. For both the strike-slip and the reverse fault sets, the σ_1 axes trend either approximately NW–SE (Fig. 5a, b) or approximately ENE–WSW (Fig. 5c, d). The NW–SE compression, which is consistent with the major fold axes of the Taiwan mountain belt, corresponds consequently to the most important deformation.

Extension (normal faults) is also present along the Lishan Fault zone. First, we found some evidence of early extensional structures, for instance, normal faults including some syn-depositional faults (Lu et al., 1991) and en échelon quartz veins which probably correspond to the tectonic evolution prior to collision. Second, a post-folding system of conjugate normal faults was recognized in a single site (Szeyuan, Fig. 6f), revealing a minor extensional NNW–SSE stress which may reflect the recent extension occurring farther north, around the Ilan Plain.

3.3. Separation and chronology of fault-slip data

Because the fault systems are complex and polyphase, particular attention had to be paid to the relative chronology of faulting. In the field, two or more types of fault-slip data were commonly found in a given site. We consequently collected data concerning crosscutting relationships between different generations of brittle structures (especially faults and veins), as well as superposed slickenside lineations indicating successive fault slips. Such sets of relative chronology data allowed distinction of tectonic events based on a matrix method (see Angelier, 1994) taking into additional account the mechanical consistency expected for each stress regime. In most cases, a given striated fault surface (or a vein) could thus be attributed to a specific tectonic regime.

An example of a polyphase site, Szeyuan (location in Fig. 2), is presented here in order to illustrate the polyphase tectonics of the Lishan Fault zone as well as the method used for separating fault-slip data (Fig. 6). At this site, different types and generations of structures were observed, including tensional quartz veins (Fig. 6a, b), two sets of strike-slip faults (Fig. 6c, d), reverse faults (Fig. 6e) and some normal faults (Fig. 6f). Several criteria of relative chronology, along with mechanical consistency, allowed separation into different tectonic regimes. These criteria are listed below.

First, superposed striations were found on some fault surfaces in several outcrops. For instance, at Szeyuan, these revealed that both the dip-slip normal faulting (Fig. 6f) and the dip-slip reverse faulting (Fig. 6e) are younger than the strike-slip faulting (Fig. 6d). This result did not constrain the chronology between normal faulting (Fig. 6f) and reverse faulting (Fig. 6e), which had to be established by different means.

Second, shear reactivation of tension gashes reveals the chronology. Some quartz veins (Fig. 6a) show later striations revealing strike slip (Fig. 6d) or reverse slip (Fig. 6e). Such observation indicates that both these strike-slip and reverse faulting events occurred later than the formation of tension gashes as quartz veins.

Third, crosscutting relationships between brittle structures are also direct indicators. Quartz veins (Fig. 6b) were found crosscut and offset by a reverse fault set (Fig. 6c), showing that reverse faulting occurred later than the development of tension gashes. Other examples include a strike-slip fault set (Fig. 6d) crosscut by a reverse fault set (Fig. 6e), and a strike-slip fault set (Fig. 6d) overprinted by a normal fault set (Fig. 6f).

Valuable, albeit indirect, chronological information is also provided by the distinction between

newly formed faults (or veins) and inherited fault slips (or vein opening). Inherited structures result from reactivation of weakness zones (such as for older faults, fractures, veins or lithological boundaries), whereas 'neoformed' ones appear during a given tectonic event. In the case of newly formed brittle features, simple geometrical relationships allow identification, whereas most inherited structures show attitudes which do not fit the mechanical requirements for most efficient shear or tension.

The relation between brittle features and folding or tilting also highlights the chronological relationships. They were useful along the Lishan Fault zone where folding is widespread (Fig. 3). At the site Szeyuan, some apparently reverse faults are in fact tilted strike-slip faults which have been rotated during folding, as shown by their geometrical relation to bedding. To illustrate this phenomenon, both the initial and present attitudes are shown in stereonets (Fig. 6c). Furthermore, these tilted strike-slip faults show a conjugate system, showing that most of them were not inherited from older events. In contrast, the other set of strike-slip faults (Fig. 6d), which does not exhibit a conjugate system, is clearly inherited (some fault surfaces are common to both these systems, with opposite senses of strike slip) and also postdates tilt. This observation highlights the consistency between the two types of indirect criteria of relative chronology.

All sources of chronological information were combined, resulting in the relationships illustrated with arrows on the right-hand side of Fig. 6. Note that double arrows indicate age relative to folding, whereas simple solid and dashed arrows indicate relative chronology at site Szeyuan and in other sites (respectively). The succession of the tectonic events was thus reconstructed as follows, from oldest to youngest (Fig. 6):

(1) A NW–SE extensional regime is revealed by a set of quartz veins (Fig. 6a) associated with few normal faults. Although we found no direct evidence that this set predated the other set of quartz veins, it probably resulted from the oldest event identified.

(2) Under a NW–SE compressional regime or a NE–SW extensional regime, many tensional quartz veins developed (Fig. 6b). This set may reflect extension along different trends relative to the earliest one, or the first occurrence of major NW–SE compression.

(3) A NE–SW compressional regime is characterized by tilted conjugate strike-slip faults (Fig. 6c). These faults now appear as oblique reverse faults at Szeyuan because they predated folding. Although this event is not a major one, its existence is beyond doubt.

(4) A NW–SE compressional regime corresponds to numerous strike-slip faults (Fig. 6d), which are generally tilted and compatible with cylindrical folding. Many of these faults are reactivated earlier faults (Fig. 6d, compare with Fig. 6c).

(5) A NW–SE compressional regime, with a trend of the σ_1 axis similar to the preceding one, is represented by reverse faults which postdate folding (Fig. 6e).

(6) A late NNW–SSE extensional regime is locally represented by a few normal faults which strike E–W or ENE–WSW (Fig. 6f).

After compilation of these different sources of information, the successions of brittle events locally identified at sites can be correlated throughout large areas, based on consistency of stress regimes and corresponding compressional or extensional trends.

3.4. Permutations of principal stress axes σ_2/σ_3

We have reconstructed a succession of deformation events and related tectonic stress states. However, because chronological criteria are scarce for some couples of events, two cases should be considered: the occurrence of distinct tectonic stress states with incompatible, mutually oblique orientations of principal stress axes (such as for Fig. 6c, d), or the existence of two different stress tensors for a single event, related by simple switches between principal stress axes (such as for Fig. 6d, e). The former case generally indicates that distinct tectonic events have occurred (see discussions in Angelier et al., 1986 for the Foothills, and Angelier et al., 1990a for the Hsüehshan Range). The latter case rather reveals minor tectonic episodes occurring under a main tectonic regime characterized by a single orientation of principal stress axes despite a permutation of principal stresses (σ_2 and σ_3 in Fig. 6d, e).

The major NW–SE compressional regime identified along the Lishan Fault zone is commonly characterized by systems of strike-slip faults, and at some sites by reverse fault systems. No well-defined

chronological relationship was found between these two systems of faults (there are relative chronologies, but they are not consistent). A simple switch between σ_2 and σ_3 stress axes accounts for this change. The abundance of such σ_2/σ_3 permutations in the Lishan Fault region suggests that although the most common expression of the widespread NW–SE compression was strike-slip faulting, this regime could easily change to a thrust tectonic regime with reverse faulting (transpression tectonics). This is in agreement with the low values (Table 2) obtained for the ratio between principal stress differences, $\Phi = (\sigma_2 - \sigma_3)/(\sigma_1 - \sigma_3)$. Thus, the transpressional tectonic regime is highly characterized by the close value between the intermediate stress σ_2 and the minimum stress σ_3.

The above characteristics of the permutation between principal stresses σ_2 and σ_3 were recognized in other areas of the Taiwan mountain belt through local stress analyses (Angelier et al., 1986, 1990a; Chu, 1990; Lee, 1994) as well as along the major faults (such as for the active Longitudinal Valley Fault, a site of oblique left-lateral reverse slip under a compressional tectonic stress regime with very low values of Φ; Angelier, 1984; Barrier and Angelier, 1986). This permutation of stress axes σ_2 and σ_3 under compressional regime is widespread for the present-day stress state in the Taiwan area, as indicated by the analysis of earthquake focal mechanisms (Yeh et al., 1991). We infer that the stress permutation phenomenon recognized along the Lishan Fault reflects a general tectonic behaviour in the Taiwan collision belt.

3.5. Results of palaeostress analysis

The results of palaeostress analysis in the Lishan Fault valley, based on calculation of reduced tensors, are summarized in Table 2. Fig. 7 shows the distribution of the calculated trends of σ_1 axes for all compressional regimes in the study area.

First, an early development of quartz veins, associated with normal faults, indicates that extension prevailed across the Chinese continental margin, prior to compression. Although no palaeostress tensor could be determined along the Lishan Fault for this early extension, this identification is consistent with many observations throughout the Taiwan mountain belt (Angelier et al., 1986, 1990a; Lu et al., 1991), and foreland area (Angelier et al., 1990b).

The NW–SE compression is by far the major tectonic event in the study area. The σ_1 axes trend N120°E on average (Fig. 7). This event is characterized not only by numerous minor faults (reverse and strike-slip) and folds (amplitudes from a few metres to tens of metres), but also by regional folds. Quartz veins are common and consistent with this NW–SE compression, despite the ambiguity mentioned above (Fig. 6b). Rather than separating reverse and strike-slip fault systems into distinct sub-events, we adopted the interpretation of multiple permutations of stress axes during a single event (see preceding section). This preference is supported by the common NW–SE trend of compression and by the absence of consistent relative chronology between the reverse and strike-slip subsets. At least the stress regimes reconstructed in Fig. 6d, e belong to this major event. This NW–SE compression belongs to the major tectonic phase which produced the principal structures of the northern Taiwan mountain belt.

In addition to this main NW–SE compression, some N–S to NNW–SSE trends of compression have been reconstructed (see Table 2 and Fig. 7, sites NIUTO002 and TULLIN02A), indicating that the Lishan Fault behaved not only as a thrust, but also seemed to undergo an oblique compression with left-lateral strike-slip (transpressional) at some stage of its tectonic evolution. The observation of outcrops of oblique thrust micro-faults in some sites also supports this argument. This NNW–SSE compression is in agreement with an older compression episode that prevailed in the northern Hsüehshan Range (Angelier et al., 1990a). Evidence in the studied area is scarce, however, and more data are required to confirm this point.

A rather enigmatic episode of NE–SW compression is characterized by conjugate systems of reverse and strike-slip faults. It played a very limited role and corresponding structures are generally minor. However, this event was undoubtedly identified at several places in Taiwan (Angelier et al., 1990a). It may be interpreted in terms of synchronous contraction sometimes occurring perpendicular to, and consistent with, the main NW–SE compression.

A N–S to NW–SE extension characterizes the most recent episode in the study area, postdating the

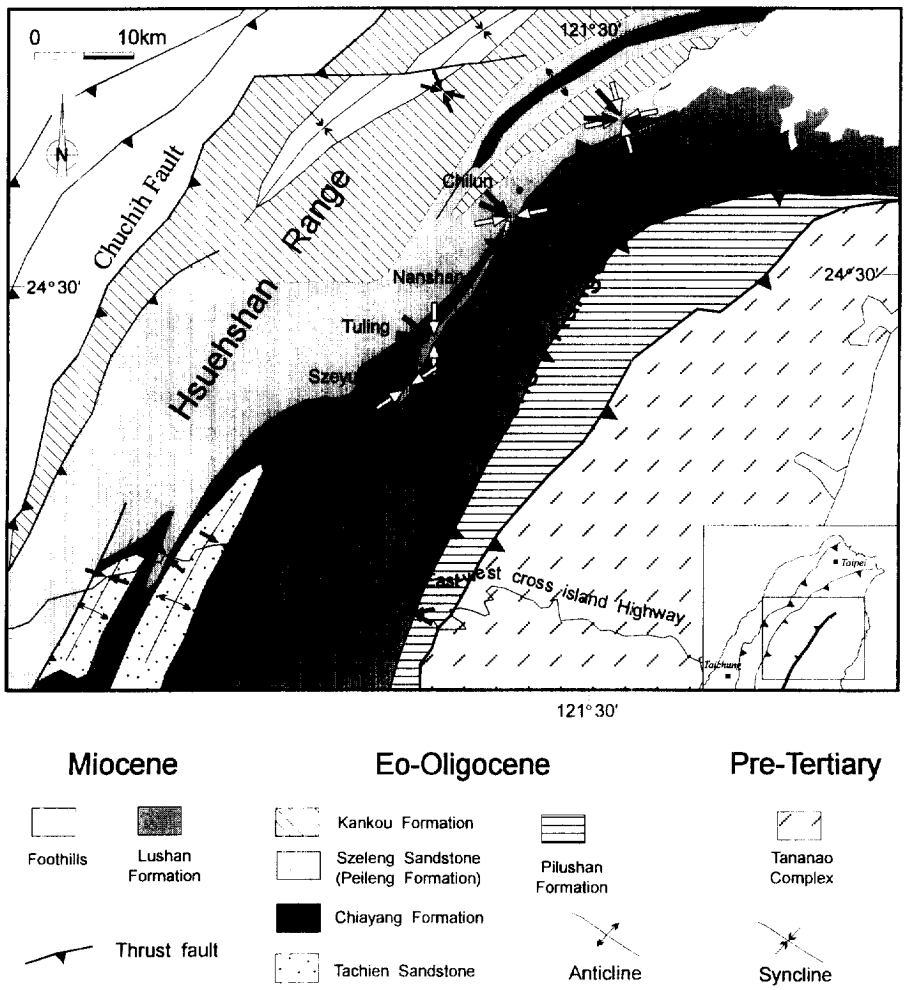

Fig. 7. Distribution of the direction of compression based on the results of palaeostress analysis in the area of the Lishan Fault. Solid arrows indicate the direction of compression (σ_1) for the major event. Open arrows refer to the minor event of WNW–ESE compression and to the occurrence of N–S compression at Tuling. Numerical results are given in Table 2.

main compressional event. Recent N–S extension is known elsewhere in northern Taiwan (Lee and Wang, 1987; Yeh et al., 1991; Lu et al., 1995).

4. Discussion and conclusion

Our tectonic analysis of the Lishan Fault zone shows that the apparent contradictions highlighted by earlier structural studies can be explained through consideration of the polyphase history.

Based on sedimentological analysis, Teng et al. (1991) and Teng (1992) proposed a half-graben structure for the Hsüehshan Range basin during the Oligocene; this interpretation seems valid for northern Taiwan only (Chu et al., 1995). The eastern limit of this half-graben structure would have been a major normal fault corresponding to the present Lishan Fault zone (Fig. 8a). During the opening of the South China Sea, which occurred in a N–S direction during the Oligocene and the Early Miocene, the continental margin including the Taiwan area was probably affected by extensional tectonics (Taylor and Hayes, 1980; Halloway, 1982; Suppe, 1988; Angelier et al., 1990b; Lu et al., 1991). As a result, faults similar to the Lishan Fault might have been reactivated as N–S-trending transcurrent faults. Both the N–S and

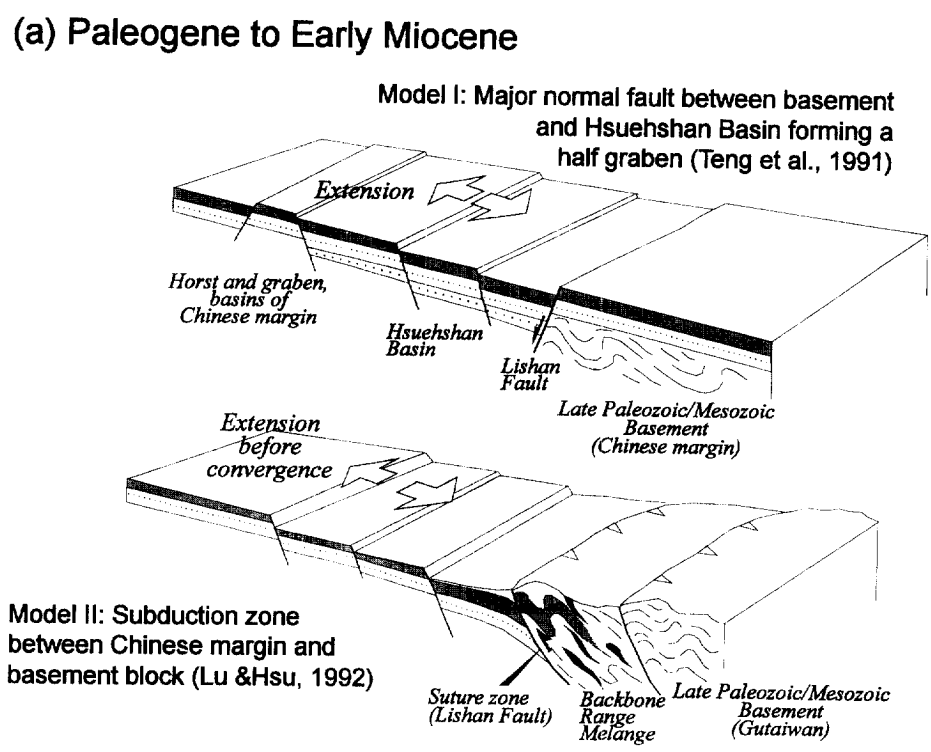
(a) Paleogene to Early Miocene
Model I: Major normal fault between basement and Hsuehshan Basin forming a half graben (Teng et al., 1991)
Extension
Horst and graben, basins of Chinese margin
Hsuehshan Basin
Lishan Fault
Late Paleozoic/Mesozoic Basement (Chinese margin)
Extension before convergence
Model II: Subduction zone between Chinese margin and basement block (Lu &Hsu, 1992)
Suture zone (Lishan Fault)
Backbone Range Melange
Late Paleozoic/Mesozoic Basement (Gutaiwan)
(b) Late Miocene - Pliocene
Reverse/Strike-slip Fault (transpression)
Lishan Fault
NNW-SSE to NW-SE compression
(c) Pleistocene
Backthrust
Lishan Fault
NW-SE to WNW-ESE compression
Uplifting
Foothills
Hsuehshan Range
Backbone Range
Meta-morphic Basement
Coastal Range

NW–SE trends of extension were identified according to palaeostress analyses in the Taiwan Strait (Angelier et al., 1990b), and the later clockwise rotation of northeastern Taiwan (Lee et al., 1991) must be taken into additional account in these comparisons, although no palaeomagnetic information is available along the Lishan Fault. Whatever the interpretation for the Oligocene–Early Miocene behaviour of the main fault zone (normal dip-slip or transcurrent), it is likely that at least on the Hsüehshan Range side many features with NE–SW general trends indicate an early extension trending approximately NW–SE, which is in general agreement with the extension which affected the Chinese continental margin during this period (Fig. 8a).

On the other hand, according to Lu and Hsü (1992), the Lishan Fault zone represents an ancient suture line of the Middle Miocene collision between the Chinese continental margin and the Gutaiwan block (Fig. 8a). This interpretation is based principally on the analysis of the Backbone Belt formations, described as a melange within a major accretionary prism. According to this interpretation, the Lishan Fault would have existed as such only since the Middle Miocene. This new reconstruction is compatible with the interpretation of the Oligocene–Early Miocene extension presented above in terms of Chinese continental margin evolution, as far as the sole western side of the Lishan Fault (the Hsüehshan Range) is concerned. This is the case for the sites which reveal early extension in the present study. It contradicts, however, the previous interpretation regarding the Backbone Range and the Lishan Fault itself (Fig. 8a).

The collision between the Philippine Sea plate and the Eurasian plate began about 5–7 Ma ago (Ho, 1986a; Teng, 1992), and was in full swing during the Plio–Quaternary (the last 5–3 Ma). During the collision and mountain building in Plio–Pleistocene time, first the Lishan Fault, a major pre-existing structure in the Tertiary strata, was probably reactivated as a west-vergent reverse fault with a (major) left-lateral strike-slip component. There is evidence for a NNW–SSE to nearly N–S compression, compatible with an increasing left-lateral component of oblique thrusting, suggesting a transpressional mechanism across the Lishan Fault (Fig. 8b).

Second, most mechanisms of folding and faulting reconstructed along the Lishan Fault zone (Figs. 6 and 7, and Table 2) belong to a major event of NW–SE to WNW–ESE compression, inducing mainly thrusting across the fault zone (Fig. 8c). Evidence for NE–SW compression is also present (Fig. 6c), but this is related to minor structures. Within the same general period of NW–SE collision, back-thrusting occurred as a late sub-event, accompanied by uplift and crustal thickening of the Hsüehshan Range, where multiple pop-up structures are present (Clark et al., 1993; Tillman and Byrne, 1995; Chu et al., 1996). During this sub-event, the east-vergent folds and flexure described earlier developed (Fig. 3). This transformation to back-thrusting of the Lishan Fault is considered a combination of the Quaternary rapid uplifting of the Hsüehshan Range and the continuation of the horizontal compression in the Taiwan mountain belt (Fig. 8c). The early stage of the Lishan Fault in west-vergent reverse and strike-slip fault (Fig. 8b) probably occurred with a steep inclination of the fault surface structure which has a mechanical tendency to turn to east-vergent thrusting near the surface during uplifting of the Hsüehshan Range.

Finally, as the mountain uplift was continuing, extensional tectonism with late normal faulting took place (Crespi, 1996; Angelier et al., 1995). Furthermore, late N–S extension occurred in the northern segment of the Lishan Fault (near the Ilan Plain), suggesting that its most recent mechanisms are influenced by the N–S back-arc opening of the Okinawa Trough northeast off Taiwan during the last 2 Ma (Letouzey and Kimura, 1985, 1986; Liu, 1995).

Fig. 8. Tectonic evolution of the Lishan Fault since the Palaeogene. (a) Palaeogene to Early Miocene. Model I with the Lishan Fault as major normal fault between the Pre-Tertiary metamorphic basement and Hsüehshan Basin, bounding a half-graben basin. Model II with the Lishan Fault as a suture zone of Miocene subduction between the Chinese continental margin (Hsüehshan Basin) and Gutaiwan block (Pre-Tertiary Basement). (b) Late Miocene to Pliocene: the Lishan Fault reactivated as oblique reverse fault with left-lateral strike-slip component. (c) Pleistocene: the Lishan Fault as east-vergent back-thrust, west-vergent thrusts dominating in the collision belt. Minor events not shown (see text).

Acknowledgements

The I.F.T.–N.S.C. cooperation framework (Institut Français à Taipei and National Science Council of Taiwan) has provided support for this work. The help of the Central Geological Survey of Taiwan, the French C.R.O.U.S, the University P. & M. Curie, the Ministry of Education of Taiwan, and the National Taiwan University is gratefully acknowledged. We wish to thank Paul Gillepsie and three anonymous reviewers for their critical points, thoughtful comments and careful reviews of this paper. This is a contribution of the Institute of Earth Sciences, Academia Sinica, IESEP 97-003.

References

Angelier, J., 1984. Tectonic analysis of fault slip data sets. J. Geophys. Res., 89: 5834–5848.

Angelier, J., 1990. Inversion of field data in fault tectonics to obtain the regional stress, III. A new rapid direct inversion method by analytical means. Geophys. J. Int., 103: 363–376.

Angelier, J., 1994. Palaeostress analysis of small-scale brittle structures. In: P. Hancock (Editor), Continental Deformation, 4. Pergamon Press, Oxford, pp. 53–100.

Angelier, J., Barrier, E. and Chu, H.T., 1986. Plate collision and paleostress trajectories in a fold–thrust belt: the Foothills of Taiwan. Tectonophysics, 125: 161–178.

Angelier, J., Bergerat, F., Chu, H.T. and Lee, T.Q., 1990a. Tectonic analysis and the evolution of a curved collision belt: the Hsüehshan Range, northern Taiwan. Tectonophysics, 183: 77–96.

Angelier, J., Bergerat, F., Chu, H.T., Juang, W.S. and Lu, C.Y., 1990b. Paleostress analysis as a key to margin extension: the Penghu Island, South China Sea. Tectonophysics, 183: 161–176.

Angelier, J., Lee, J.C., Chu, H.T., Lu, C.Y., Fournier, M., Hu, J.C., Lin, N.T., Deffontaines, B., Delcaillau, B., Lacombe, O. and Lee, T.Q., 1995. Crustal extension in an active orogen: Taiwan. Int. Conf. 3rd Sino–French Symp. Active Collision in Taiwan, Progr. Extended Abstr., pp. 25–32.

Barrier, E. and Angelier, J., 1986. Active collision in eastern Taiwan: the Coastal Range. Tectonophysics, 125: 39–72.

Biq, C., 1971. Some aspects of post-orogenic block tectonics in Taiwan. Recent crustal movements. Bull. R. Soc. N.Z., 9: 19–24.

Chang, L.S., 1971. A biostratigraphic study of the so-called slate formation in Taiwan based on smaller Foraminifera, I. The E–W cross-mountain highway. Proc. Geol. Soc. China, 14: 45–61.

Chang, L.S., 1974. A biostratigraphic study of the so-called slate formation in Taiwan based on smaller foraminifera, IV. Northernmost part of the Central Range of Taiwan. Proc. Geol. Soc. China, 17: 85–93.

Chang, L.S., 1976. The Lushanian Stage in the Central Range of Taiwan and its fauna. In: Y. Takaganagi and T. Saito (Editors), Progress in Micropaleontology. Micropaleontology Press, New York, pp. 27–35.

Chen, C.H., 1977. Some stratigraphic problems of the Hsüehshan Range of Taiwan. Proc. Geol. Soc. China, 20: 61–70.

Chen, C.H., 1979. Geology of the east–west cross-island highway in central Taiwan. Mem. Geol. Soc. China, 3: 219–236.

Chen, C.H., 1984. Determination of lower greenschist facies boundary by K–mica–chlorite crystallinity in the Central Range, Taiwan. Proc. Geol. Soc. China, 27: 41–53.

Chen, C.H., 1992. Problems of stratigraphic correlations in the Hsüehshan and Central Ranges of Taiwan (in Chinese). Spec. Publ. Cent. Geol. Surv., 6: 39–68.

Chen, C.H., Chu, H.T. and Chuang, T.Y., 1983a. Some structural problems of the Central Range of Taiwan (in Chinese). Bull. Cent. Geol. Surv., 2: 1–16.

Chen, C.H., Chu, H.T., Liou, H.G. and Ernst, W.G., 1983b. Explanatory notes for the metamorphic facies map of Taiwan. Spec. Publ. Cent. Geol. Surv., 2, 32 pp.

Chu, H.T., 1990. Néotectonique cassante et collision plio-quaternaire à Taiwan. Mém. Sci. Terre Univ. P. & M. Curie, Paris, 292 pp.

Chu, H.T., Hu, H.N., Liew, H.T. and Chuang, T.Y., 1995. The geology of the western slope of the Nantawushan, southern Taiwan. Bull. Cent. Geol. Surv., 10: 1–22.

Chu, H.T., Lu, C.Y. and Lee, J.C., 1996. Crustal thickening in the fold-and-thrust belt: an example of mountain building in the Hsüehshan Range, Central Taiwan (abstr.). 30th International Geological Conference, Beijing.

Clark, M.B., Fisher, D.M., Lu, C.Y. and Chen, C.H., 1993. Kinematic analyses of the Hsüehshan Range, Taiwan: a large-scale pop-up structure. Tectonics, 1: 205–217.

Crespi, J., 1996. Deformation partitioning at shallow crustal levels in the Taiwan arc–continent collision. J. Geol. Soc. China., 39(2): 143–150.

Crespi, J., Chan, Y.C. and Swaim, M., 1996. Synorogenic extension and exhumation of the Taiwan hinterland. Geology, 24(3): 247–250.

Dunne, W.M. and Hancock, P.L., 1994. Palaeostress analysis of small-scale brittle structures. In: P. Hancock (Editor), Continental Deformation, 5. Pergamon Press, Oxford, pp. 101–120.

Dupin, J.-M., Sassi, W. and Angelier, J., 1993. Homogeneous stress hypothesis and actual fault slip: a distinct element analysis. J. Struct. Geol., 15(8): 1033–1043.

Halloway, N.H., 1982. North Palawan Block, Philippines—Its relation to Asian Mainland and role in evolution of South China Sea. Am. Assoc. Pet. Geol. Bull., 63: 1355–1383.

Ho, C.S., 1986a. A synthesis of the geologic evolution of Taiwan. Tectonophysics, 125: 1–16.

Ho, C.S., 1986b. Geological Map of Taiwan, 1 : 500,000. Cent. Geol. Surv., MOEA, Taipei.

Ho, C.S., 1988. An introduction to the geology of Taiwan: explanatory text of the geology map of Taiwan, 2nd ed., Ministry of Economic Affaires, Taipei, 192 pp.

Hsieh, X.L., 1990. Fisson-track dating of zircons from several east–west cross-sections of Taiwan island (in Chinese).

Unpublished M.S. thesis, National Taiwan Univ., Taipei.

Huang, C.S. and Lee, C.F., 1992. Sedimentary environments of the Meichi Sandstone and its contact relationship with the Szeleng Sandstone, Hsüehshan Range (in Chinese). Spec. Publ. Cent. Geol. Surv., 6: 143–152.

Lee, J.F., 1987. Preliminary study on paleo-stress of Tachien Sandstone, Chinshan to Techi (in Chinese). Master thesis, National Taiwan University, Taipei.

Lee, J.C., 1994. Structure et déformation active d'un orogène: Taiwan. Mém. Sci. Terre Univ. P. & M. Curie, Paris, 281 pp.

Lee, C.T. and Wang, Y., 1987. Paleostress change due to the Pliocene–Quaternary arc–continent collision in Taiwan. Mem. Geol. Soc. China, 9: 63–86.

Lee, T.Q., Angelier, J., Chu, H.T. and Bergerat, F., 1991. Rotations in the northern eastern collision belt of Taiwan: preliminary results from paleomagnetism. Tectonophysics, 199: 109–120.

Letouzey, J. and Kimura, M., 1985. The Okinawa Trough genesis, structure and evolution of a back-arc basin developed in a continent. Mar. Pet. Geol., 2: 111–130.

Letouzey, J. and Kimura, M., 1986. The Okinawa Trough: genesis of a back-arc basin developing along a continental margin. Tectonophysics, 125: 209–230.

Liou, J.G., 1981. Recent high CO_2 activity and Cenozoic progressive metamorphism. Mem. Geol. Soc. China, 4: 551–581.

Liu, T.K., 1988. Fission track dating of the Hsüehshan Range: Thermal record due to arc–continent collision in Taiwan. Acta Geol. Taiwanica, 26: 279–290.

Liu, C.C., 1995. The Ilan Plain and the southwestward extending Okinawa Trough. J. Geol. Soc. China, 38(3): 229–242.

Lu, C.Y. and Hsü, K.J., 1992. Tectonic evolution of the Taiwan mountain belt. Pet. Geol. Taiwan, 27: 21–46.

Lu, C.Y., Lee, J.C. and Lee, J.F., 1991. Extension and compression tectonics in central Taiwan. In: J. Cosgrove and M. Jones (Editors), Neotectonics and Resources. Belhaven Press, London, pp. 85–92.

Lu, C.Y., Angelier, J., Chu, H.T. and Lee, J.C., 1995. Contractional, transcurrent, rotational and extensional tectonics: a case study in northern Taiwan. Tectonophysics, 246: 129–146.

Petit, J.P., 1987. Criteria for the sense of movement on fault surfaces in brittle rocks. J. Struct. Geol., 9: 597–608.

Suppe, J., 1988. Tectonics of arc–continent collision on both sides of the South China Sea: Taiwan and Mindoro. Acta Geol. Taiwanica, 26: 1–18.

Taylor, B. and Hayes, D.E., 1980. The tectonic evolution of the South China basin. In: D.E. Hayes (Editor), The Tectonic and Geologic Evolution of Southeast Asian Seas and Islands. Am. Geophys. Union Geophys. Monogr., 22: 98–104.

Teng, L.S., 1992. Geotectonic evolution of Tertiary continental margin basins of Taiwan. Pet. Geol. Taiwan, 27: 1–19.

Teng, L.S., Wang, Y., Tang, C.H., Huang, T.C., Yu, M.S. and Ke, A., 1991. Tectonic aspects of the Paleogene deposition basin of northern Taiwan. Proc. Geol. Soc. China, 34(4): 313–336.

Tillman, K. and Byrne, T., 1995. Kinematics analysis of the Taiwan slate belt. Tectonics, 14(2): 322–341.

Tsai, Y.B., 1975. Correlation between microearthquakes and geologic faults in the Hsintien–Ilan area. Pet. Geol. Taiwan, 12: 149–168.

Tseng, C.S., 1978. Geology and geothermal occurrence of the Chingshui and Tuchang districts, Ilan (in Chinese). Pet. Geol. Taiwan, 15: 11–23.

Wu, F.T., 1978. Recent tectonics in Taiwan. J. Phys. Earth, 26: S265–S299.

Yeh, Y.H., Barrier, E., Lin, C.H. and Angelier, J., 1991. Stress tensor analysis in the Taiwan area from focal mechanisms of earthquakes. Tectonophysics, 200: 267–280.